

## INORGANIC CHEMISTRY

UDC 54.18+532.785

<https://doi.org/10.31489/2021Ch2/31-42>

S.M. Asadov\*

*Institute of Catalysis and Inorganic Chemistry ANAS, Baku, Azerbaijan*  
(\*Corresponding author's e-mail: [salim7777@gmail.com](mailto:salim7777@gmail.com))

### Modeling of nonlinear processes of nucleation and growth of $\text{GaS}_x\text{Se}_{1-x}$ ( $0 \leq x \leq 1$ ) solid solutions

The results on the study of modeling and physico-chemical study of the kinetics of nucleation and growth of  $\text{GaS}_x\text{Se}_{1-x}$  ( $0 \leq x \leq 1$ ) solid solution. The nucleation heterogeneous process and growth of  $\text{GaS}_x\text{Se}_{1-x}$  crystals have been studied and simulated taking into account nonlinear equations considering the kinetic behavior of crystallizing phases.  $\text{GaS}_x\text{Se}_{1-x}$  single and nanocrystals were grown from solution, melt, and by chemical transport reaction through steam.  $\text{GaS}_x\text{Se}_{1-x}$  crystals were grown by chemical transport reaction in a two-temperature gradient furnace in a sealed quartz ampoule. Iodine was used as a transporting additive. Using the Fokker–Planck equation, the evolution of the distribution function of crystals of solid solutions of the GaS–GaSe system by size at the nucleation time is studied by a numerical method. For the convenience of comparing theory with experimental data, we used the  $\text{GaS}_{1-x}\text{Se}_x$  ( $x = 0.7$  molar fraction of GaSe) composition of the solid solution. The Monte Carlo method is used to approximate the time evolution of the nucleation of two types of particles for the  $\text{GaS}_{0.3}\text{Se}_{0.7}$  solid solution, simulated by a constant nucleus size. The results of modeling nonlinear crystallization processes are consistent with experimental data.

*Keywords:* nonlinear modeling, kinetics equation of crystallization, semiconductor  $\text{GaS}_{1-x}\text{Se}_x$  solid solutions, numerical solution algorithm, finite-difference equations, Fokker–Planck equation, evolution of the distribution function, Monte Carlo method.

#### Introduction

The optical properties of the synthesized semiconductor two-dimensional (2D) nanocrystals have prospects for use in devices of quantum electronics (optical elements and switches, transistors, modulators, etc.). The functional capabilities of these devices are determined, in particular, by such parameters of nanocrystals as the average radius, band gap, and component composition.

The processes of nucleation and crystal growth are known to be difficult to predict, describe and control [1]. They are associated with the temporary existence of nanoparticles, making them difficult to quantify. After the formation of nuclei, their growth is observed. In this case, the growth conditions may differ from the initial stages of nucleation. In addition, during experimental crystallization, several technologically interacting processes can operate [2].

This article discusses the processes of nucleation and the subsequent formation and growth of layered crystals of 2D  $\text{GaS}_x\text{Se}_{1-x}$  solid solutions [3, 4]. In particular, we consider the GaS–GaSe semiconductor system consisting of a highly volatile inorganic melt, and the process of nonlinear nucleation and crystallization. This situation can arise during crystallization, when trying to obtain small crystals of semiconductor solid solutions and compounds.

Interest in semiconductor materials based on  $\text{A}^{\text{III}}\text{B}^{\text{VI}}$  compounds, which are characterized by quantum effects, is due to the potential for their use in nanoscale devices. Data on the crystal and electronic structure of GaS and GaSe compounds are given in [5, 6]. GaS and GaSe crystals belong to hexagonal syngony, characterized by a layered structure and space group  $D_{3h}^1 - P\bar{6}m2$  [6]. They have several polymorphic modifications.

For example, GaSe has four modifications ( $\beta$ -,  $\varepsilon$ -,  $\gamma$ - and  $\delta$ -GaSe). At room temperature  $\beta$ -GaS and  $\varepsilon$ -GaSe are more thermodynamically stable modifications.

In  $A^{III}B^{VI}$  crystals covalent bonds are in the layers, and a weak Van der Waals bond exists between the layers. Due to this anisotropic properties manifest in  $A^{III}B^{VI}$ . By their optical and electrical properties  $A^{III}B^{VI}$  crystals (GaS [7], GaSe [8]) are close to promising nanotechnology materials, such as graphene and topological insulators. GaS and GaSe are wide-gap semiconductors and at room temperature have a band gap of 2.53 and 1.98 eV, respectively. They have several advantages over other  $A^{III}B^{VI}$  materials: a large range of operating temperatures, the possibility to create light-emitting devices on their basis in the visible spectrum, high values of the critical field of electrical breakdown, radiation resistance.

GaS and GaSe form a continuous series of  $GaS_xSe_{1-x}$  ( $0 \leq x \leq 1$ ) solid solutions between each other [9, 10]. However, the formed poly- and single crystals of  $GaS_xSe_{1-x}$  solid solutions often have an inhomogeneous distribution of dislocation density, which leads to mechanical stresses and the formation of intrinsic point defects [11–14]. As a result, such a material has irreproducible electrical, optical, photoelectric, luminescent, and other physical characteristics.

The reasons for the nonuniform distribution of structural defects over the volume of the formed  $GaS_xSe_{1-x}$  crystals are determined by several processes. The main ones are crystallization (edge and screw dislocations, grain boundaries, pores can form) and heat treatment of crystals (point defects intrinsic and impurity can be created or eliminated), as a result of which concentration and temperature gradients appear. However, the dimensional and kinetic parameters phases affecting the structure formation and physical properties of  $GaS_xSe_{1-x}$  have not yet been considered.

In the present work the crystallization of  $GaS_xSe_{1-x}$  solid solutions is considered, taking into account metastable phases, which are formed by fluctuations. The results of studying the crystallization of  $GaS_xSe_{1-x}$  in a closed system are presented. Nonlinear crystallization processes of  $GaS_xSe_{1-x}$  are considered in the framework of the Fokker–Planck type equation [15] in the size space. The evolution of the two-dimensional distribution of kernels of different types in the  $GaS_xSe_{1-x}$  melt is modeled using the Monte Carlo method [16].

### Experimental

The elements Ga-5 N gallium, B5 sulfur and OSCh-17-3 selenium with impurity content no higher than  $5 \times 10^{-4}$  mass% were used in the synthesis of GaS and GaSe binary compounds. Syntheses of GaS and GaSe compounds were performed by melting the initial elements taken in stoichiometric ratios in evacuated ( $10^{-3}$  Pa) quartz ampoules. The ampoules with the corresponding components were placed in an electric furnace for synthesis. At temperatures above the melting point of GaS and GaSe (melting points of GaS and GaSe are 1288 and 1211 K, respectively), ampoules may be destroyed due to high vapor pressure of chalcogens. The ampoules were held for 6–8 h at a temperature 5–10 K above the melting point of the compounds. Then ampoules with liquid components GaS and GaSe were cooled in the power off mode to room temperature. The  $GaS_xSe_{1-x}$  solid solutions were prepared in a similar way. Synthesized GaS (GaSe) compounds and  $GaS_xSe_{1-x}$  solid solutions were identified by differential thermal analysis (DTA; a heating/cooling rate of  $10 \text{ K min}^{-1}$ ) and powder X-ray diffraction analysis (XRD). DTA of GaS (GaSe) compounds and  $GaS_xSe_{1-x}$  solid solutions was carried out using a NETZSCH 404 F1 Pegasus system. The accuracy of measurements was  $\pm 0.5$  to 1 K. The XRD phase composition of the obtained samples was performed on a Bruker D8 ADVANCE diffractometer with the Cu K-alpha radiation [10].

When crystallizing a substance from a solution, as it is known, the solute undergoes transition from the liquid phase to the crystalline phase. This process is accompanied by the appearance of many small single crystals (mass crystallization). Mass crystallization was performed by cooling a supersaturated  $GaS_xSe_{1-x}$  solution with the subsequent simultaneous formation of many crystallization centers.  $GaS_xSe_{1-x}$  single crystals were grown from solution, melt, and by chemical transport reaction through steam [17, 18].

When growing from a melt the ampule was moved in the furnace at a rate of  $0.5\text{--}1.1 \text{ mm}\cdot\text{h}^{-1}$ , and the temperature gradient near the crystallization front was  $25 \pm 3 \text{ K}$ .  $GaS_xSe_{1-x}$  crystals were grown during chemical transport reaction in a two-temperature gradient furnace in a sealed quartz ampoule. Iodine was used as a transporting additive.

A homogenized solid solution quenched in the concentration region of the  $T-x$  phase diagram of the GaS–GaSe system may remain in the metastable state for some time. Ultimately, it reaches thermodynamic equilibrium. At one of the equilibrium concentrations, some micro clusters can form in the matrix  $GaS_xSe_{1-x}$  [19, 20].

*Fokker–Planck equation.* The kinetics of nucleation in the GaS–GaSe system was studied by an equation of the Fokker–Planck type [15]. This equation allows to describe the dynamics of changes in certain crystallization properties, considering the properties to be random walk. The equation allows to consider the evolution of the size distribution function and to describe the walk of nuclei in the size space. In other words, the Fokker–Planck equation characterizes diffusion with the presence of a drifting force field. It describes the evolution in time of the probability density function of the particle’s position, which follows the stochastic differential equation. In this case, sample particle trajectories are continuous functions of time. Such a model is used in this work.

Within the framework of this model, we assume that crystallization is described by an equation based on the evolution of the function  $\varphi_k$  of the crystal size distribution ( $L$ ) in time ( $t$ ). In the entire volume of the solution, the temperature and concentration are constant. Then the Fokker–Planck kinetic equation for the distribution density is written as

$$\frac{\partial \varphi}{\partial t} = -\frac{\partial(\varphi G)}{\partial L} + \frac{\partial}{\partial L} \left( p \frac{\partial(\varphi G)}{\partial L} \right), \quad (1)$$

where  $L \geq L_0$ ;  $L_0$  is the minimum crystal size;  $G$  is the linear growth rate of the crystal face, and  $p$  is the fluctuation coefficient of the growth rate.

The supersaturation of a solution is determined as follows:  $\gamma(t) = C_k(t) / C_k^\infty$ , where  $C_k(t)$  is the concentration in time  $t$ ,  $C_k^\infty$  is the concentration of the saturated solution. Here the linear velocity is  $G = \beta(\gamma - 1)$ , where  $\beta$  is the kinetic coefficient of the growth rate.

The system of nonlinear equations was solved numerically, where a uniform grid was used with a step  $h$  in size and  $t$  in time. The solution was transferred from the  $j$ -th layer to the  $(j+1)$ -st layer by a purely implicit difference scheme, after this the function  $G$  was recalculated. The differencing scheme for equation (1) has the form:

$$\frac{\varphi_i^{j+1} - \varphi_i^j}{\tau} = -\frac{G^j}{2h} (\varphi_{i+1}^{j+1} - \varphi_{i-1}^{j+1}) + \frac{pG^j}{h^2} (\varphi_{i+1}^{j+1} - 2\varphi_i^{j+1} + \varphi_{i-1}^{j+1}). \quad (2)$$

Equation (2) has order of approximation  $O(\tau + h^2)$ . The difference equation for the left boundary condition has the form

$$\varphi_0^{j+1} G^j - pG^j \frac{\varphi_1^{j+1} - \varphi_0^{j+1}}{h} + pG^j \frac{\varphi_0^j 2\varphi_1^j + \varphi_2^j}{h^2} = \eta^j. \quad (3)$$

The equation has order of approximation  $O(\tau + \tau h + h^2)$ . Difference equations were solved by the sweep method, which is applicable due to diagonal prevalence. The differencing schemes (2) and (3) are stable on the right-hand side. After transferring the solution to the  $(j+1)$ -st layer, a new value of the concentration  $C_k$  was calculated, as well as parameters  $G$  and  $\eta$ . The integral was calculated by the trapezoidal rule — its accuracy is of the order of  $O(h^2)$ , which corresponds to the approximation of the differencing scheme. The obtained concentration value  $C_k$  was reused to find the solution on the  $(j+1)$ -st layer. This procedure was repeated a fixed number of times. Thus, the crystallization of a multicomponent system is considered as a combination of physico-chemical and mathematical models. Such a model allows for the numerical implementation of nonlinear equations by a differencing scheme. Numerical experiments to study the crystallization of  $\text{GaS}_x\text{Se}_{1-x}$  were carried out in Delphi software.

*Monte Carlo Simulation.* Known models of the crystal growth process with their own microphysics allow to describe homogeneous and heterogeneous nucleation and growth with two separate one-dimensional size distributions. With this approach, the model allows to approximate only the average mass of a heterogeneous solution contained in growth units of a certain size. In this case it is impossible to track the spectral distribution of the mass of the heterogeneous solution in growth units.

The evolution of the two-dimensional distribution of phase characteristics during the growth of  $\text{GaS}_x\text{Se}_{1-x}$  by transport chemical reactions was simulated by the stochastic algorithm [Gillespie (1976) [21]] for chemical reactions using the Monte Carlo method [22]. Within the framework of this algorithm, the set of a discrete one-component kinetic equation is defined as:

$$\frac{\partial N(m, n; t)}{\partial t} = \frac{1}{2} \sum_{m'=0}^m \sum_{n'=0}^n K(m-m', n-n'; m', n'; t) N(m-m', n-n'; t) N(m', n'; t) - N(m, n; t) \sum_{m'=0}^m \sum_{n'=0}^n K(m, n; m', n') N(m', n'; t), \quad (4)$$

where  $N(m, n; t)$  is the average number of particles consisting of  $m$  and  $n$  monomers of the first and second kind, respectively.

A continuous version of this equation is known, for example, in the form of Laurenzi et al. [23]:

$$\frac{\partial N(m, n, t)}{\partial t} = \frac{1}{2} \int_0^m dm' \int_0^n dn' K(m-m', n-n'; m', n') N(m-m', n-n'; t) N(m', n'; t) - N(m, n; t) \int_0^m dm' \int_0^n dn' K(m, n; m', n') N(m', n'; t), \quad (5)$$

where  $K(m, n; m', n')$  in (4) and (5) is a constant set of nuclei, which now depends on the composition of coagulating particles.

Discrete equation (4) gives the temporal rate of change in the average number of a polycrystalline monomer with mass  $m$  and a single crystal monomer with mass  $n$  as the difference of two terms, the first term gives a gain in the number of particles whose polycrystal mass has a size  $m$ , and a single crystal mass has a size  $n$ .

The equation is calculated as the sum of binary clusters between monomers: one with the mass of a polycrystal from the phase of size  $m'$  and the mass of a single crystal from the phase of size  $n'$ , and the other with the mass of a polycrystal from the phase  $m-m'$  and the mass of a single crystal from the phase  $n-n'$ . The second contribution describes the average rate of depletion  $(m, n)$  of particles due to their fusion with particles of other types. To solve equations (4) and (5) the following initial conditions are required:

$$N(m, n; 0) = N_0(m, n) \quad (6)$$

For a discrete equation for any  $t$  it is also possible to take  $N(0, 0; t) = 0$ . The numerical solution for (4) and (5) is complicated because of the double integral and nonlinear behavior of these equations. The nonlinearity of the equation, in particular during the growth of  $\text{GaS}_x\text{Se}_{1-x}$ , is associated with the nature of the interaction of nuclei and growth cells of a single crystal with different masses in each of them.

### Results and Discussion

Figure 1 shows X-ray powder diffraction patterns of  $\text{GaS}_x\text{Se}_{1-x}$  solid solutions and  $\beta$ -GaS and  $\beta$ -GaSe pure compounds, which crystallize in hexagonal syngony with the space group  $P6_3/mmc$  and have the following lattice parameters:  $\beta$ -GaS ( $a = 4.002 \pm 0.002 \text{ \AA}$  and  $c = 15.447 \pm 0.005 \text{ \AA}$ ) and  $\beta$ -GaSe ( $a = 3.755 \pm 0.002 \text{ \AA}$  and  $c = 15.475 \pm 0.005 \text{ \AA}$ ) at room temperature.

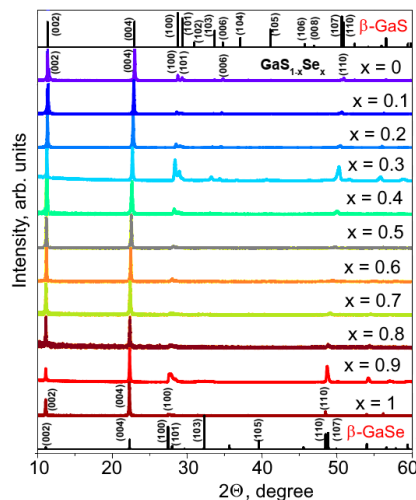
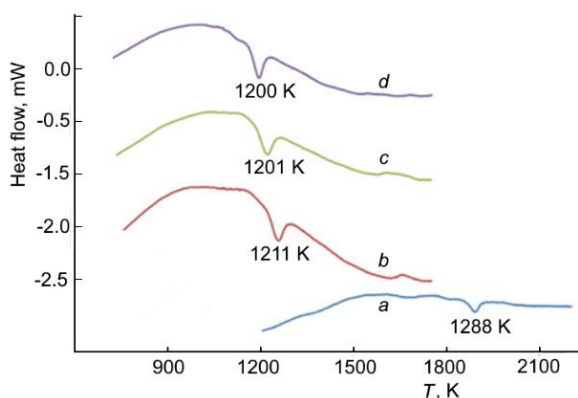


Figure 1. XRD patterns of  $\beta$ -GaS (top),  $\beta$ -GaSe (bottom) and solid solutions  $\text{GaS}_{1-x}\text{Se}_x$  at 298 K

These values of lattice parameters of for polytypes  $\beta$ -GaS and  $\beta$ -GaSe compounds are consistent with the literature data [10, 11] and the JCPDS-ICDD Powder Diffraction File (PDF) card file data:  $\beta$ -GaS (JCPDS No: 30-0576;  $a = 3.587 \text{ \AA}$  and  $c = 15.492 \text{ \AA}$ ),  $\beta$ -GaSe (JCPDS No: 03-65-3508;  $a = 3.7555$  and  $c = 15.94 \text{ \AA}$ ). The values of lattice constants of  $\text{GaS}_x\text{Se}_{1-x}$  solid solutions are also consistent with the data of [10, 11].

The difference between the structural parameters can be explained with the degree of purity of the components used, the experimental procedure and calculation of the lattice parameters, as well as the polytypicity of the GaS and GaSe compounds. The number of formula units in the lattice and the density of the compounds were as follows:  $Z = 4$ ;  $\rho_e = 3.87 \text{ g/cm}^3$ ,  $\rho_r = 3.89 \text{ g/cm}^3$  (for GaS) and  $Z = 4$ ;  $\rho_e = 5.03 \text{ g/cm}^3$ ,  $\rho_r = 5.07 \text{ g/cm}^3$  (for GaSe).

According to the XRD (Fig. 1) data and DTA (Fig. 2), the components of GaS and GaSe unlimitedly dissolve in each other both in the liquid and in the solid state. Unlimited component solubility in GaS–GaSe occurs because both GaSe and GaS have the same crystal structure, and Se and S have similar radii, electronegativity and valence. In GaSe–GaS system melting occurs over a relatively narrow temperature range between the solidus and liquidus lines. In other words, solid and liquid phases are at equilibrium in a narrow temperature range.



*a* — GaS; *b* —  $x = 0.8$ ; *c* —  $x = 0.7$  mole fraction GaSe; *d* — GaSe

Figure 2. Differential thermal analysis curves of solid solutions  $\text{GaS}_{1-x}\text{Se}_x$  crystals

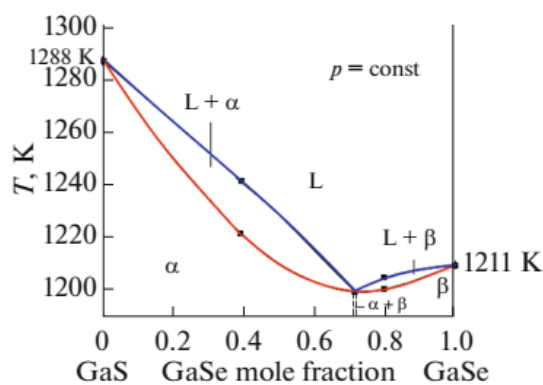


Figure 3. Calculated (curves) and experimental (dots) phase diagram in GaS–GaSe system

According to DTA and DSC data for components GaSe and GaS, the following melting parameters were chosen:  $\Delta H^m$  (GaSe) =  $30300 \pm 200 \text{ J mol}^{-1}$ ,  $T^m$  (GaSe) =  $1211 \pm 3 \text{ K}$ ,  $\Delta H^m$  (GaS) =  $34800 \pm 200 \text{ J mol}^{-1}$ , and  $T^m$  (GaS) =  $1288 \pm 3 \text{ K}$ . Comparison of these data with experimental data [10] indicates their correspondence.

On the basis of DTA, XRD and thermodynamic calculation, the equilibrium  $T$ – $x$  phase diagram of the GaS–GaSe quasibinary system with unlimited component solubility is described and modeled (Fig. 3). The phase diagram of the quasi-binary system GaS–GaSe is characterized with unlimited solubility of the components in the liquid and solid states. Crystallization and melting curves have a minimum point at a composition of about 70 mol % GaSe.

Model takes into consideration our experimental thermodynamic data on the initial GaS and GaSe components. The concentration–temperature dependence of the Gibbs free energy of mixing of  $\text{GaS}_x\text{Se}_{1-x}$  solid solutions, calculated taking into account the rule of mixing components, well approximates the  $T$ – $x$  phase diagram of the GaS–GaSe system. Conductivity smoothly changes with a change in the composition of solid solutions  $\text{GaS}_x\text{Se}_{1-x}$  ( $x = 0$ – $1$  mole fraction) single crystals. As the concentration of selenium in solid solutions increases, their conductivity also gradually increases by about two orders of magnitude at 298 K.

Calculated solidus and liquidus temperatures differ slightly from the experimental data (solidus difference was  $\sim 5 \text{ K}$  and liquidus  $\sim 10 \text{ K}$ ). Phase diagram of the state for GaS–GaSe system is characterized by the minimum ( $0.7 \pm 0.05$  mol fraction GaSe and  $1200 \pm 1 \text{ K}$ ) and presence of unlimited mutual solubility of the components in the system.

Our calculation and experimental DTA data on the temperatures of liquidus, solidus and the coordinates of the invariant equilibria in the GaS–GaSe system are extremely different from the old data given in [9]. The melting point of GaSe is 1210 K [24], which exactly  $\pm 1$  K matches our data.

A study of the relief of  $\text{GaS}_{1-x}\text{Se}_x$  crystals grown of various compositions indicates the formation of various two-dimensional (2D) nanostructures on the surface [19, 20]. Two main types of heterogeneities can be distinguished: extended structures and local 2D nano-objects.

$\text{GaS}_x\text{Se}_{1-x}$  solid solutions melt without decomposition and have no phase transitions. Depending on the composition of  $\text{GaS}_x\text{Se}_{1-x}$ , the physical properties of solid solutions differ noticeably.

The mathematical model used by us describes the nucleation in the dispersed region of the melt, deposition in the homogeneous phase region, transfer of monomers between the two regions, formation and subsequent growth of crystals in both regions. The model was composed as a system of coupled nonlinear differential equations. The number of particles of all types present was fixed and stored, which allows to ignore the description of the nucleation rate. Moreover, it is possible to analyze each process step by step.

For convenience of comparison with the experimental data we used the  $\text{GaS}_{1-x}\text{Se}_x$  ( $x = 0.7$  molar fraction of GaSe) composition of the solid solution in the simulation.  $\text{GaS}_{0.7}\text{Se}_{0.3}$  corresponds to the minimum in the GaS–GaSe phase diagram and can be considered as a quasi-one-component.

When deposition occurs in a homogeneous phase region, the concentration of monomers falls below the equilibrium concentration at the surface of the droplets in the dispersed region. This leads to the transfer of monomers from the droplets to the homogeneous region. Then the homogeneous phase is incorporated into crystals and nuclei, i.e., a single crystal is grown. In this case, the presented numerical calculations, taking into account the sizes and/or masses of particles, agree with the experimental data.

*Nucleation.* The evolution of the dispersed phase in crystallization experiments in a closed system occurs by a complex mechanism. In this case, the formation of metastable intermediate solid phases and the evolution of dispersed particles of the solid phase at the end of the process are possible. The mechanisms of such phase transformations and the crystallization kinetics are described using nonlinear models [25, 26]. Nonlinear properties of the crystallization process are determined taking into account the boundary conditions and coefficients of the kinetic equations, and also depend on the crystallization prehistory. Kinetic coefficients are calculated based on the theory of diffusion growth and dissolution of second-phase precipitates. These coefficients determine the probability of attachment and ejection of one particle per unit time, respectively.

A homogenized solid solution quenched in the concentration region of the  $T$ – $x$  phase diagram of the GaS–GaSe system [10] can remain in a metastable state for some time. Ultimately, it reaches thermodynamic equilibrium. At one of the equilibrium concentrations, some microclusters can form in the  $\text{GaS}_x\text{Se}_{1-x}$  matrix [19, 20].

Taking into account the 2D nucleation mechanism [26], the growth of single crystal can be represented as follows. Crystal faces grow due to the formation of two-dimensional nuclei of critical size in the absence of screw dislocations ending on the surface. 2D nuclei are formed when individual growth units (for example, atoms, molecules, dimers) are adsorbed on the surface of a crystal, diffuse and agglomerate. After a 2D nucleus becomes larger than its critical size, it becomes thermodynamically advantageous for attaching growth units to this nucleus. In a supersaturated solution a 2D nucleus larger than the critical one propagates across the face until it reaches the crystal boundary. These boundaries can be either the edge of the crystal layer, or the front of the layer below it or the growth front from another nucleus.

The nucleation rate  $J(t)$  approaches a stable state according to an equation of the form [27]

$$J(t) = J_s \left[ 1 - \exp(-t / t_{lag}) \right] \\ 1 / (6.3a(L_c)Z^2) \geq t_{lag} \geq 1 / (12a(L_c)Z^2), \quad (7)$$

where  $J_s$  is the stationary nucleation rate;  $Z$  is the Zeldovich factor;  $a(L_c)$  is the rate at which monomers are absorbed by a cluster with a critical size  $L_c$ ;  $t_{lag}$  is the time lag.

This expression (7) describes the asymptotic behavior of the Fokker–Planck equation and is in qualitative agreement with the numerical calculation for the dependence of the nucleation frequency of  $\text{GaS}_x\text{Se}_{1-x}$  on time. Since the gradient ( $L$ ) in the region  $|L - L_c| < 1/2Z$  is small, the cluster will move in this region by random walk with a jump frequency  $a(L_c)$ . The time required for the cluster to disperse the  $1/Z$  distance by random walk is determined by the time lag, which is estimated as  $t_{lag} = 1 / 2a(L_c)Z^2$ .

Using Fokker–Planck equation. Suppose that crystallization of solid solutions occurs from a uniformly supersaturated solution in a closed system. Solution has a limited volume  $V$  at time  $t = 0$ . If the concentration of the dispersed phase  $Q$  exceeds the solubility of the components of the system, then the nucleation and growth of the solid phase occurs. With such crystallization, the formation of various modifications of the solid phase is possible.

Assume that during crystallization a chemical reaction does not occur and a constant temperature of the solution is maintained. Mixing the solution does not lead to cracking and aggregation. Mass crystallization occurs by spontaneous nucleation, i.e., nucleation of crystallization centers, crystal growth and dissolution of particles of the dispersed phase.

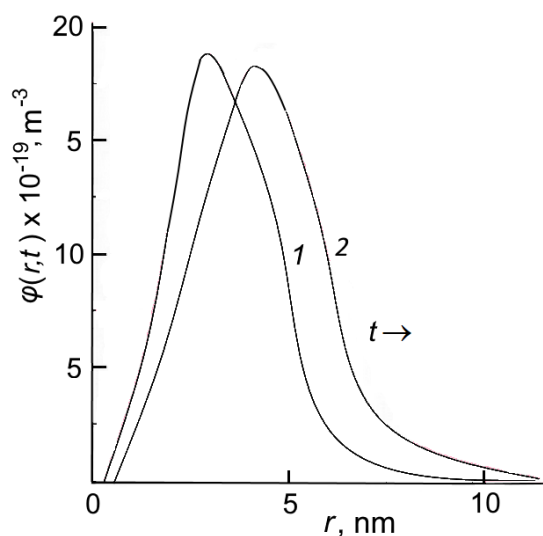
Nucleation involves the formation and growth of clusters from molecules of the initial solution. Cluster formation occurs up to the size at which it is possible to distinguish a crystal face as a structural element responsible for growth. The nucleation rate, crystal growth rate and dissolution of the particles of the dispersed phase are determined with the degree of supersaturation of the solution and the size of the crystal face [28, 29].

Since the formed crystals have a limited size, it is necessary to choose the boundary conditions for the equation of distribution density. After that, the kinetic equation is supplemented by the initial condition and the balance equation. Thus, we obtain a system of nonlinear equations that are solved by the difference method [30].

The Fokker–Planck equation approximates distribution density of  $\text{GaS}_x\text{Se}_{1-x}$  crystals by size (Fig. 4a). It was assumed that the temperature dependence on nanocrystals (particle) size is described by the relation

$$T = T_0 \exp\left(\frac{R^2}{R_0^2}\right), \quad (8)$$

where  $R$  is the particle radius;  $R_0$  is the initial particle radius.



1 — 0.005 and 2 — 0.001. Curve — approximation by dependence (1) at  $\gamma = 5$  and  $\beta = 1$  (Equation (1))

Figure 4a. Evolution of distribution function of  $\text{GaS}_{0.3}\text{Se}_{0.7}$  solid solution by size in nucleation time ( $t$ , s)

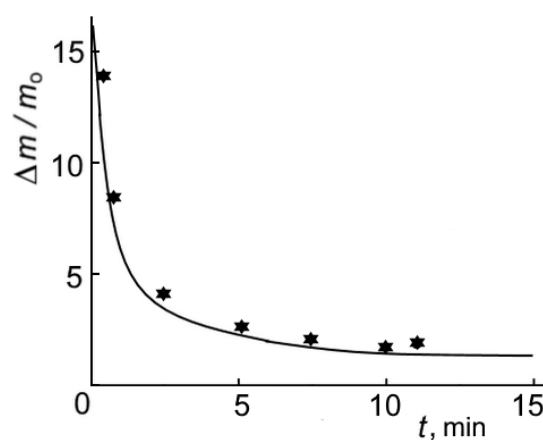


Figure 4b. Relative mass dependence of  $\text{GaS}_{0.3}\text{Se}_{0.7}$  nanocrystal on time;  $m$  is particle mass with diameter  $d \approx 30$  nm,  $m_0$  is arithmetic mean mass of particles

Comparison results of the calculation (curve) and experiment (points) of the dynamics of the mass change ( $\Delta m$ ) of  $\text{GaS}_x\text{Se}_{1-x}$  nanocrystals with respect to the initial arithmetic mean mass of particles  $m_0$  diameter  $\sim 30$  nm are shown in Figure 4b. Numerical experiments indicate that the concentration of crystals of a given composition varies from the initial supersaturation to equilibrium concentration in a very short time. From the concentration dependence of the formed  $\text{GaS}_x\text{Se}_{1-x}$  crystals on the formation time, it follows that the bulk of the crystals is formed within  $2 \times 10^{-3}$  s from the moment of crystallization initiation.

At the same time, the crystal concentration of a given composition decreases from the initial supersaturation to the equilibrium concentration. This process is accompanied by a decrease in the oversaturation of the solution. The supersaturation ends with a constant number of nuclei and then the crystals grow with a further

increase in crystal size. Thus, when using the Fokker–Planck equation, the concentration of the crystallizing phase was taken into account, as well as data on the supersaturation and crystal size.

*Using the stochastic model by the Monte Carlo method.* Within the framework of the stochastic model [21–23] we consider a spatially homogeneous volume  $V$ , in which there are particles belonging to  $N_s$  different types of particles. Each type is characterized by both its liquid mass and the mass of its nucleus,  $\bar{u}_\mu = (u_m, u_n)$ . Let us assume that the forming particle with the composition  $\bar{u}_\mu$  is a member of the  $\mu$ -type. After time  $t = 0$  the types can be randomly combined according to the reaction  $A_{m,n} + B_{m',n'} = C_{m+m',n+n'}$ , where  $A_{m,n}$  and  $B_{m',n'}$  are particles of composition  $\bar{u}_\mu = (u_m, u_n)$  and  $\bar{u}_v = (u_{m'}, u_{n'})$ , respectively.

According to this model, the transition probabilities for particle merging events are:

$$a(i, j) = V^{-1} K(i, j) n_i n_j dt \equiv P(i, j; t) dt, \quad (9)$$

where  $K(i, j)$  is the set of nuclei;  $V$  is the volume of the solution.

$P(i, j; t) dt$  – Pr is the probability that two particles of  $i$  and  $j$  (for  $ij$ ) types with  $n_i$  and  $n_j$  number of particles will collide in the nearest time interval. Then the probability of collision of two particles of the same type  $i$  with the number of particles  $n_i$  during the inevitable time interval can be represented in the form

$$a(i, i) = V^{-1} K(i, i) \frac{n_i(n_i - 1)}{2} dt \equiv P(i, i; t) dt. \quad (10)$$

Within this structure the  $\mu$  index is possible for each pair of nuclei  $i, j$  that can collide. For a system with  $N$  types  $(S_1, S_2, \dots, S_N)$   $v \in N \frac{(N+1)}{2}$ . The set  $\{v\}$  defines the total collision space and is equal to the total number of possible interactions. Then the probabilities of  $\alpha(i, j)$  and  $\alpha(i, i)$  transitions can be represented by one index  $(\alpha_v)$ .

This stochastic model for  $\text{GaS}_x\text{Se}_{1-x}$  crystallization was solved using an algorithm introduced by Gillespie [21] for chemical kinetics and modified by Laurenzi et al. [23].

*Comparison of Monte Carlo simulations with experimental data.* The evolution of the two-dimensional distribution of nuclei (crystal nucleus) during crystal growth was simulated using the Monte Carlo method. A stochastic algorithm for chemical reactions was used to simulate the kinetic behavior of the nuclear distribution. A set of two-component kinetic equations was used.

The performance of stochastic Monte Carlo simulation (MCS) was tested by studying the growth of crystals with a constant nucleus size in solution, and the results were compared with our experimental data on the kinetics of nucleation. The influence of a two-component set of nuclei on the dynamics of mass fluctuations of nuclei of the process was studied.

To simulate random processes associated with the deviation of the types of nuclei from the critical size, the Monte Carlo method was used. Time evolution of particle species was approximated based on the distribution of the output value  $N(y)$ , where  $N$  is the number of particle types,  $y$  is the type of particle nuclei. For random  $f(m, t)$  and  $f(n, t)$ , the equations for  $N$  are stochastic differential equations. Therefore the statistical description of the growth process was carried out using kinetic collection equations for two corresponding probability distributions.

In MCS the number of particles of a certain critical size grown from a solution in their original form, i.e., the initial number of particles was taken as  $\leq 60$ , and the average value was calculated for 1000 realizations taking into account the dynamic distribution of particles.

For simulation of a two-component constant of a discrete set of nuclei, the following value was used:  $K(m, n; m', n') = 1.1 \times 10^{-4} \text{ cm}^3 \text{ s}^{-1}$ . The monomer particle had a radius of  $10 \mu\text{m}$  (particle mass  $m_0 = 3.77 \times 10^{-9} \text{ g}$ ), and the dispersed monomer was a solid-liquid (SL)  $\text{GaS}_x\text{Se}_{1-x}$  with a radius of  $0.1 \mu\text{m}$  (mass of the SL phase  $n_0 = 7.11 \times 10^{-15} \text{ g}$ ). The mass grid of the SL-solution was selected in accordance with the mass of the particle  $(i) = i \times m_0$ ,  $(i = 1, \dots, N_p)$  and the mass of the SL phase  $(j) = j \times n_0$ ,  $(j = 1, \dots, N_{s-1})$ .

The volume of the studied system in all calculations was taken to be  $1 \text{ cm}^3$ . 30 intervals for the particle mass grid and 30 intervals for the SL phase mass grid were determined. We also took into account the

possibility of the existence of pure monomeric particles containing pure GaS and/or GaSe particles, as well as pure structural units of SL GaS and SL GaSe. Then the total number of types in our numerical experiment can be calculated as:  $N_{\text{total}} = N_p \times N_{s-1} + N_p + N_{s-1}$ .

The maximum number of types of structural units that can be generated during simulation, in the selected case, is 960. Solutions obtained as a result of Monte Carlo calculations for  $N(1, 1; t)$ ,  $N(1, 0; t)$  and  $N(0, 1; t)$  types are shown in Figure 5a–c. Our experimental data are also shown in Figure 5.

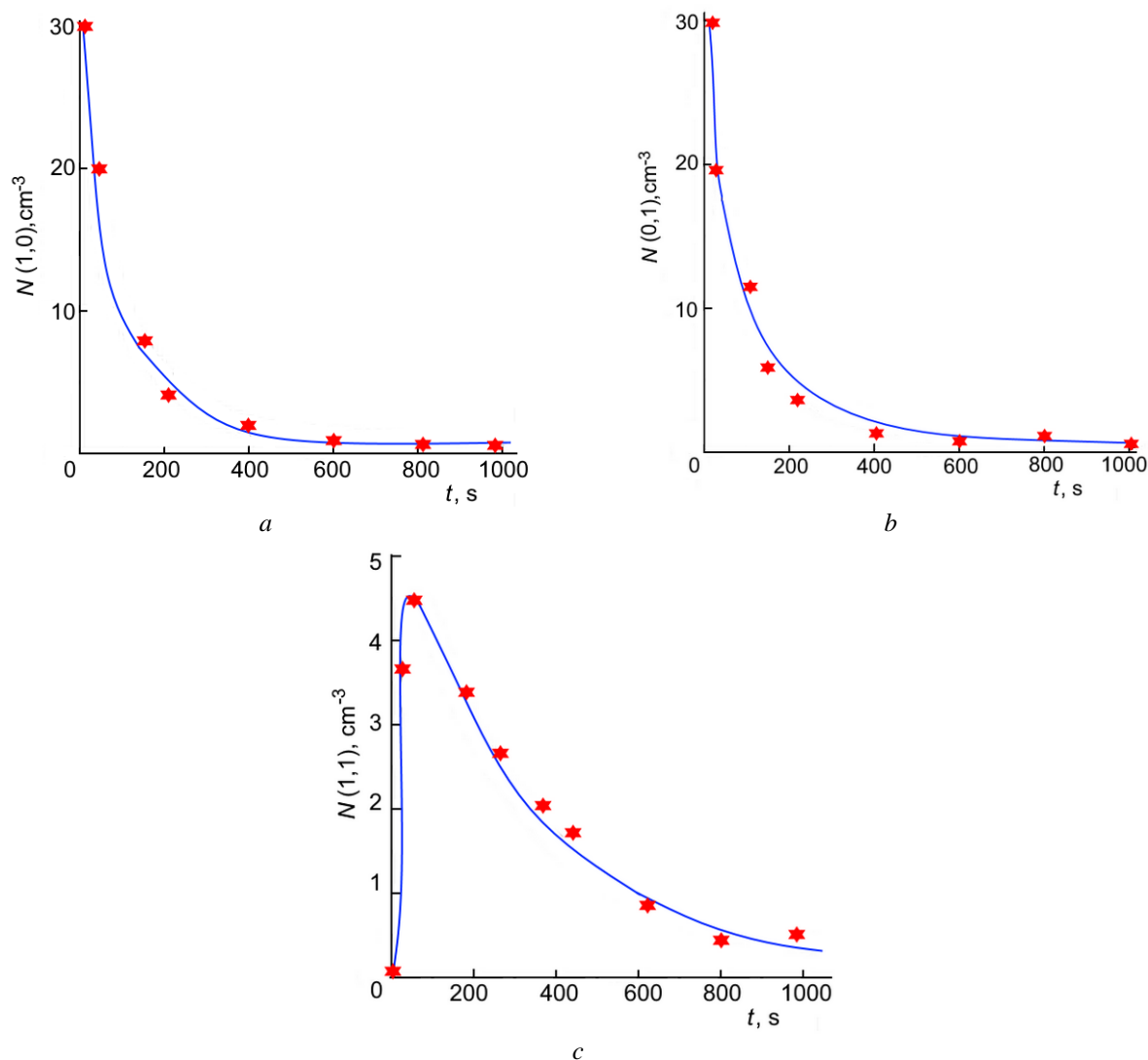


Figure 5. Modeling of time evolution of the types of nanocrystals (a)  $N(1, 0)$ , (b)  $N(0, 1)$ , and (c)  $N(1, 1)$  for a  $\text{GaS}_{0.3}\text{Se}_{0.7}$  solid solution modeled by a constant nucleus size (a solid phase nucleus in a melt)  $K(m, n; m', n') = 1.1 \times 10^{-4} \text{ cm}^3 \text{ s}^{-1}$ . Approximation curve are the result of Monte Carlo simulation of the two-component kinetic equation (5). Approximation curve of the averaging result over 1000 realizations

The differences between the mean values of Monte Carlo simulations and experimental data are negligible and they can be substantiated by statistical criteria. Description of the two-dimensional discrete size distribution after 100 s also indicates agreement between the mean values of the Monte Carlo simulation and the experimental data.

### Conclusions

We used a model close to the ideal solid solution  $\text{GaS}_x\text{Se}_{1-x}$ , which resembles the structure of the liquid phase. A set of self-consistent thermodynamic parameters was obtained. The calculated phase diagram and thermodynamic property data were in good agreement with the experimental information. In the GaS–GaSe

system, the existence of continuous  $\text{GaS}_x\text{Se}_{1-x}$  solid solutions and the formation of a phase diagram with a minimum at 70 mol% GaSe were confirmed.

Model of kinetics of  $\text{GaS}_x\text{Se}_{1-x}$  nucleation using the Fokker–Planck equation takes into account compositional fluctuations due to the initial state of solid solutions. It was established that taking into account random walks into the size space during crystallization allows to describe the dynamics of changes in the  $\text{S}_x\text{Se}_{1-x}$  properties.

By numerically solving the equation, the evolution of the size distribution function of the  $\text{GaS}_x\text{Se}_{1-x}$  crystal nuclei in nucleation time is approximated. For calculations a purely implicit differencing scheme is used, which involves splitting the extended volume of the solution into independent fragments. It follows from the time dependence of the concentration of  $\text{GaS}_x\text{Se}_{1-x}$  crystals ( $x = 0.7$ ) that the bulk of the crystals was formed within  $2 \times 10^{-3}$  s from the moment of crystallization initiation.

The multicomponent Monte Carlo algorithm based on a stochastic approach to chemical reactions, using the example of  $\text{GaS}_x\text{Se}_{1-x}$  allowed to calculate statistical fluctuations for two-component aggregation of particles taking into account their radius and composition. Taking into account the transition probability in microphysical processes allows to determine how a specific pair of particles (nuclei, crystals, solid-liquid) with a set of properties will be aggregated in the next time interval.

The solution of the continuous set of the kinetic equation shows that if an individual particle acquires a mass much greater than the rest of the system, then it is necessary to take into account statistical fluctuations in the region of large particle masses. Agreement between the numerical solutions of Monte Carlo simulations and experimental data on crystal growth in the GaS–GaSe system was observed.

The variety of stationary distributions for time evolution of the types of structural units indicates the possibility of controlling the process of two-component aggregation of nuclei by varying the properties of the nuclei of a pair of particles during the formation of crystals of given sizes.

## References

- 1 *Nucleation in Condensed Matter: Applications in Materials and Biology*. (2010). K.F. Kelton and A.L. Greer (Eds.). Pergamon Materials Series 15. Amsterdam. Elsevier. Pergamon. 726 p. ISBN: 9780080421476
- 2 Sangwal, K. (2018). *Nucleation and Crystal Growth. Metastability of Solutions and Melts*. John Wiley & Sons, Inc. 479 p. ISBN 9781119461586
- 3 Asadov, S.M. (2020). Modeling of crystallization of a 2D  $x\text{GaS}-(1-x)\text{GaSe}$  solid solutions taking into account fluctuation // *Abstracts Book. XVI International Conference on Thermal Analysis and Calorimetry in Russia. RTAC-2020*. June 6th. Online. Moscow, Russia. P. 31.
- 4 Asadov, S.M., Mustafaeva, S.N., & Lukichev, V.F. (2020). Modeling of the Crystallization and Correlation of the Properties with the Composition and Particle Size in Two-Dimensional  $\text{GaS}_x\text{Se}_{1-x}$  ( $0 \leq x \leq 1$ ). *Russian Microelectronics*, 49(6), 452–465. <https://doi.org/10.1134/S1063739721010042>
- 5 Vasil'ev, V.P. (2007). Correlations between the thermodynamic properties of II–VI and III–VI phases. *Inorganic Materials*, 43(2), 115–124. <https://doi.org/10.1134/S0020168507020045>
- 6 *Semiconductors Data Handbook*. (2004). Madelung O., Ed. Berlin: Springer <https://doi.org/10.1007/978-3-642-18865-7>
- 7 Mustafaeva, S.N., & Asadov, M.M. (1983). Currents of isothermal relaxation in  $\text{GaS}\langle\text{Yb}\rangle$  single crystals. *Solid State Communications*, 45(6), 491–494. [https://doi.org/10.1016/0038-1098\(83\)90159-X](https://doi.org/10.1016/0038-1098(83)90159-X)
- 8 Mustafaeva, S.N., & Asadov, M.M. (1986). High field kinetics of photocurrent in GaSe amorphous films. *Materials Chemistry and Physics*, 15, 185–189. [https://doi.org/10.1016/0254-0584\(86\)90123-9](https://doi.org/10.1016/0254-0584(86)90123-9)
- 9 Rustamov, P.G. (1967). *Khalkogenidy galliia [Gallium chalcogenides]*. Baku: Academy of Sciences of the AzSSR [in Russian].
- 10 Asadov, S.M., Mustafaeva, S.N., & Mammadov, A.N. (2018). Thermodynamic assessment of phase diagram and concentration–temperature dependences of properties of solid solutions of the GaS–GaSe system. *Journal of Thermal Analysis and Calorimetry*, 133(2), 1135–1141. <https://doi.org/10.1007/s10973-018-6967-7>
- 11 Ho, C.H., Wang, S.T., Huang, Y.S., & Tiong, K.K. (2009). Structural and luminescent property of gallium chalcogenides  $\text{GaSe}_{1-x}\text{S}_x$  layer compounds. *J. Mater. Sci. Mater. Electron*, 20, 207–210. <https://doi.org/10.1007/s10854-007-9539-3>
- 12 Bereznyaya, S., Korotchenko, Z., Redkin, R., Sarkisov, S., Tolbanov, O., & Trukhin, V. et al. (2017). Broadband and narrowband terahertz generation and detection in  $\text{GaSe}_{1-x}\text{S}_x$  crystals. *J. Opt.*, 19, 115503. <https://doi.org/10.1088/2040-8986/aa8e5a>
- 13 Kolesnikov, N.N., Borisenko, E.B., Borisenko, D.N., Tereshchenko, A.N., & Timonina, A.V. (2018). Synthesis and Growth of  $\text{GaSe}_{1-x}\text{S}_x$  ( $x = 0-1$ ) Crystals from Melt. Phase Composition and Properties. *Inorganic Materials: Applied Research*, 9(1), 66–69. <https://doi.org/10.1134/S2075113318010173>
- 14 Wang, T., Li J., Zhao, Q., Yin, Z., Zhang, Y., & Chen, B. et al. (2018). High-Quality GaSe Single Crystal Grown by the Bridgman Method. *Materials*, 11(2), 186. <https://doi.org/10.3390/ma11020186>
- 15 Risken, H. (1996). *The Fokker–Planck equation: methods of solutions and applications*, 2nd Edn. Springer-Verlag. Berlin. Heidelberg. 486 p. <https://doi.org/10.1007/9783642615443>

- 16 Landau, D.P., & Binder, K. (2003). *A Guide to Monte Carlo Simulations in Statistical Physics*. Cambridge University Press. 384 p. ISBN 0521 653142
- 17 Li, X., Lin, M.W., Poretzky, A.A., Idrobo, J.C., Ma, C., & Chi, M., et al. (2014). Controlled vapor phase growth of single crystalline, two-dimensional GaSe crystals with high photoresponse. *Sci. Rep.*, 4, 5497. <https://doi.org/10.1038/srep05497>
- 18 Mustafaeva, S.N., Asadov, M.M., Kyazimov, S.B., & Gasanov, N.Z. (2012). T-x phase diagram of the TlGaS<sub>2</sub>-TlFeS<sub>2</sub> system and band gap of TlGa<sub>1-x</sub>Fe<sub>x</sub>S<sub>2</sub> (0 ≤ x ≤ 0.01) single crystals. *Inorganic Materials*, 48(10), 984–986. <https://doi.org/10.1134/s0020168512090117>
- 19 Kokh, K.A., Molloy, J.F., Naftaly, M., Andreev, Yu.M., Svetlichnyi, V.A., & Lanskiy, G.V., et al. (2015). Growth and optical properties of solid solution crystals GaSe<sub>1-x</sub>S<sub>x</sub>. *Mater. Chem. Phys.*, 154, 152–157. <https://doi.org/10.1016/j.matchemphys.2015.01.058>
- 20 Borisenko, E., Borisenko, D., Bdikin, I., Timonina, A., Singh, B., & Kolesnikov, N. (2019). Mechanical characteristics of gallium sulfide crystals measured using micro- and nanoindentation. *Materials Science and Engineering: A*, 757, 101–106. <https://doi.org/10.1016/j.msea.2019.04.095>
- 21 Gillespie, D.T. (1976). A general method for numerically simulating the stochastic time evolution of coupled chemical reactions. *Journal of Computational Physics*, 22(4), 403–434. [https://doi.org/10.1016/0021-9991\(76\)90041-3](https://doi.org/10.1016/0021-9991(76)90041-3)
- 22 Tzivion, S., Reisin, T.G., & Levin, Z. (1999). A Numerical Solution of the Kinetic Collection Equation Using High Spectral Grid Resolution: A Proposed Reference. *Journal of Computational Physics*, 148, 527–544. Article ID jcph.1998.6128
- 23 Laurenzi, I.J., Bartels, J.D., & Diamond, S.L. (2002). A General Algorithm for Exact Simulation of Multicomponent Aggregation Processes. *Journal of Computational Physics*, 177(2), 418–449. <https://doi.org/10.1006/jcph.2002.7017>
- 24 Zheng, F., Shen, J.Y., Liu, Y.Q., Kim, W.K., Chu, M.Y., & Ider, M., et al. (2008). Thermodynamic optimization of the Ga–Se system. *CALPHAD*, 32(2), 432–438. <https://doi.org/10.1016/j.calphad.2008.03.004>
- 25 Kashchiev, D. (2003). *Nucleation. Basic Theory with Applications*. 1st Ed. Butterworth-Heinemann, Oxford. Amsterdam. Elsevier. 551 p. ISBN: 9780750646826
- 26 Kalikmanov, V.I. (2013). *Nucleation Theory*. Springer Science+Business Media Dordrecht. ISBN 978-90-481-3642-1
- 27 Saito, Y., Honjo, M., Konishi, T., & Kitada, A. (2000). Time-Dependent Nucleation Rate. *Journal of the Physical Society of Japan*, 69(10), 3304–3307. <https://doi.org/10.1143/jpsj.69.3304>
- 28 Horsta J.H., & Kashchiev D.J. (2005). Determining the nucleation rate from the dimer growth probability. *Chem. Phys.*, 123(11), 114507. <https://doi.org/10.1063/1.2039076>
- 29 Michael, A.L., Andrea, R.B., Derek, W.G., Jacob, P.S., Ryan, C.S., & Michael, F.D. (2008). Crystal Shape Engineering. *Ind. Eng. Chem. Res.*, 47(24), 9812–9833. <https://doi.org/10.1021/ie800900f>
- 30 Jovanović, B.S., & Süli, E. (2014). *Analysis of Finite Difference Schemes*. 46. Springer-Verlag, London. <https://doi.org/10.1007/978-1-4471-5460-0>

C.M. Асадов

### GaS<sub>x</sub>Se<sub>1-x</sub> (0 ≤ x ≤ 1) қатты ерітіндісінің ядролануы мен өсуінің сызықтық емес процестерін модельдеу

GaS<sub>x</sub>Se<sub>1-x</sub> (0 ≤ x ≤ 1) қатты ерітіндісінің ядролануы мен өсу кинетикасын модельдеу және физика-химиялық зерттеулердің нәтижелері келтірілген. GaS<sub>x</sub>Se<sub>1-x</sub> кристалдарының ядролануы мен өсуінің гетерогенді процесі зерттеліп, кристалдану фазаларының кинетикалық әрекетін ескеретін сызықтық емес теңдеулерді ескере отырып, модельденді. GaS<sub>x</sub>Se<sub>1-x</sub> монокристалдары мен нанокристалдары ерітіндіден, балқымадан және химиялық бу беру реакциясы арқылы өсірілді. GaS<sub>x</sub>Se<sub>1-x</sub> кристалдары химиялық тасымалдау реакциясы әдісімен герметикалық кварц ампуласында екі температуралы градиент пешінде алынды. Йод тасымалдаушы қоспа ретінде пайдаланылған. Фоккер-Планк теңдеуін қолдана отырып, GaS–GaSe жүйесінің қатты ерітінділерінің кристалдарының үлестіру функциясының эволюциясы сандық әдіспен зерттелді. Теорияны тәжірибелік мәліметтермен салыстыруға ыңғайлы болу үшін GaS<sub>1-x</sub>Se<sub>x</sub> қатты ерітіндісінің құрамы қолданылды (x = 0,7 молярлық фракция GaSe). Монте-Карло әдісі GaS<sub>0,3</sub>Se<sub>0,7</sub> қатты ерітіндісі үшін бөлшектердің екі түрінің ядролануының уақыт эволюциясын жақындату үшін пайдаланылған, тұрақты ядро өлшемімен модельденген. Сызықтық емес кристалдану процестерін модельдеу нәтижелері тәжірибелік мәліметтермен сәйкес келеді.

*Кілт сөздер:* сызықтық емес модельдеу, кристалдану кинетикасының теңдеуі, GaS<sub>1-x</sub>Se<sub>x</sub> қатты жартылай өткізгіштері, сандық шешімдердің алгоритмі, ақырлы айырымдық теңдеулер, Фоккер-Планк теңдеуі, үлестіру функциясының эволюциясы, Монте-Карло әдісі.

С.М. Асадов

**Моделирование нелинейных процессов зарождения и роста твердых растворов  $\text{GaS}_x\text{Se}_{1-x}$  ( $0 \leq x \leq 1$ )**

Приведены результаты исследования моделирования и физико-химического исследования кинетики зарождения и роста твердого раствора  $\text{GaS}_x\text{Se}_{1-x}$  ( $0 \leq x \leq 1$ ). Гетерогенный процесс зародышеобразования и роста кристаллов  $\text{GaS}_x\text{Se}_{1-x}$  изучен и смоделирован с учетом нелинейных уравнений, учитывающих кинетическое поведение кристаллизующихся фаз. Монокристаллы и нанокристаллы  $\text{GaS}_x\text{Se}_{1-x}$  были выращены из раствора, расплава и путем химической реакции переноса через пар. Кристаллы  $\text{GaS}_x\text{Se}_{1-x}$  получены методом химической транспортной реакции в двухтемпературной градиентной печи в запаянной кварцевой ампуле. Йод использовался в качестве транспортной добавки. С помощью уравнения Фоккера-Планка численным методом изучена эволюция функции распределения кристаллов твердых растворов системы GaS–GaSe по размерам в момент зарождения. Для удобства сравнения теории с экспериментальными данными применялся состав твердого раствора  $\text{GaS}_{1-x}\text{Se}_x$  ( $x = 0,7$  мольная доля GaSe). Метод Монте-Карло использовался для аппроксимации временной эволюции зарождения двух типов частиц для твердого раствора  $\text{GaS}_{0,3}\text{Se}_{0,7}$ , моделируемого постоянным размером зародыша. Результаты моделирования нелинейных процессов кристаллизации согласуются с экспериментальными данными.

*Ключевые слова:* нелинейное моделирование, уравнение кинетики кристаллизации, полупроводниковые твердые растворы  $\text{GaS}_x\text{Se}_{1-x}$ , алгоритм численного решения, конечно-разностные уравнения, уравнение Фоккера–Планка, эволюция функции распределения, метод Монте-Карло.

## Information about author:

**Asadov, Salim M.** (contact person) — Candidate of technical sciences, Senior researcher, Azerbaijan National Academy of Sciences, Institute of Catalysis and Inorganic Chemistry, AZ1143 Baku, H. Cavid ave. Azerbaijan; e-mail: [salim7777@gmail.com](mailto:salim7777@gmail.com); <https://orcid.org/0000-0001-7146-728X>